β-Delayed Proton Decays in the Rare-Earth Region Near Drip Line*

XU Shu-Wei[1)]　LI Zhan-Kui　XIE Yuan-Xiang　GUO Wen-Tao

(Institute of Modern Physics, Chinese Academy of Sciences, Lanzhou 730000, China)

Abstract　The history of experimental study on β-delayed proton decays in the rare-earth region was simply reviewed. The physical results of the β-delayed proton decays obtained at IMP, Lanzhou over the last 10 years were summarized, mainly including the first observation of 9 new β-delayed proton precursors along the odd-Z proton drip line and the new data for 2 waiting-point nuclei in the rp-process. The results were compared and discussed with different nuclear model calculations. Finally, the perspective in near future was briefly introduced.

Key words　β-delayed proton decay, rare-earth region, proton drip line, waiting point nuclei

1　Historical review

First study on β-delayed proton (βp) decay in rare-earth region was made by Bogdanov et al at Dubna in 1977[1]. The studied isotopes, such as ^{135}Sm, ^{133}Sm, ^{129}Nd and ^{131}Nd, were produced via the fusion evaporation reaction induced by heavy ion beam ^{32}S. An ISOL facility named BEMS-2 with a surface ionization ion source was employed to identify the isotopes. In 1984 the β-delayed decays of ^{145}Dy, ^{147}Dy, ^{147}Er and ^{149}Er were observed for the first time by D. Schardt et al at GSI[2], where ^{58}Ni beam and GSI mass separator with a FEBIAD ion source were used in their experiment. During the period from 1983 to 1993 a remarkble progress was reported by Nitschke and Wilmarth et al at LBL[3—11] because of following technical improvements. The surface ionization ion source in combination with the OASIS ISOL could work at the temperature higher than 2800℃. A cooling target system was constructed so as to the low melting-point targets and high beam intensity could be used. Different heavy ion beams, including ^{36}Ar, ^{40}Ca, ^{54,56}Fe, ^{58,60}Ni and ^{64}Zn, were available. Finally, more than 30 β-delayed proton decays in the rare-earth region were observed for the first time at LBL (see Fig. 1). However, up to 1995 the magin line of known β-delayed proton precursors in the rare-earth region could not reach the odd-Z proton drip line Z=0.743N+11.6 predicted by Hofmann[12].

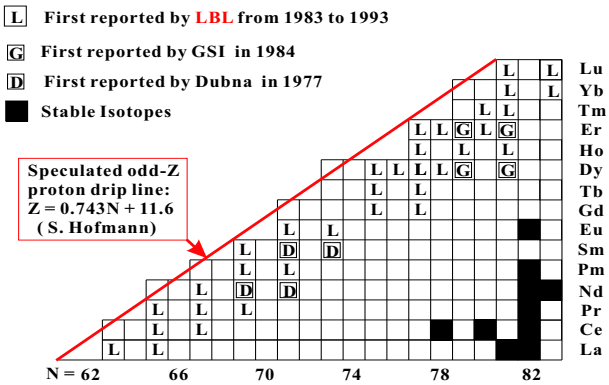

Fig. 1.　Chart of the rare-earth nuclides on neutron deficient side before 1995.

One of the difficulties encountered in the study of continuous-energy βp near the drip line is caused by the isobaric contaminations. In order to identify a βp precursor unambiguously, besides a mass separation,

* Supported by National Natural Science Foundation of China (10375078)

1) E-mail: xsw@impcas.ac.cn

additional measurements, such as "x-p" coincidence, i.e., the coincidence between the characteristic x rays of the proton emitter and the βp, have to be carried out. However, due to the low branching ratio of the electron capture (EC), the "x-p" coincidence measurements will reduce the counting rate by one or two orders of magnitude . This fact severely constrains the study of a βp channel with the production cross section as low as 100nb, and leads us to use a different technique to identify the βp precursor instead.

2 Experimental procedure

The experiments were carried out at the Sector-Focusing Cyclotron in the Institute of Modern Physics, Lanzhou, China.. The ^{32}S, ^{36}Ar or ^{40}Ca beam with the energies of 5—6MeV/amu from the cyclotron entered a target chamber filled with 1-atm. helium, passing through a 1.89mg/cm^2 thick Havar window, and finally bombarded a metal target with the thickness about 2.0mg/cm^2, such as ^{92}Mo, ^{96}Ru, ^{106}Cd or ^{112}Sn. The low melting-point targets ^{106}Cd and ^{112}Sn were mounted on a copper wheel which was surrounded with a cooling device and could be rotated. Using a He-jet the reaction products were then swept through a teflon capillary, 6.0 m long and 2 mm in diameter, and implanted in the movable tape in a collection chamber. After a certain period of collection, the activity on the tape was transported to a shielded counting room for p-γ_1(x)-γ_2(x)-t coincidence measurements. While the first activity sample was being counted, the next one was being collected. Two 570mm^2×350μm totally depleted silicon surface barrier detectors were used for proton measurements, and located on two opposite sides of the movable tape. Behind each silicon detector there was a coaxial HpGe(GMX) detector for γ(x) measurements. Energy and time spectra of γ(x) ray and proton were taken in coincidence mode.

3 Improvement of identification

In the EC/β decay of an even(Z)-odd(N) βp precursor, most of the excited-state decays in the even($Z-2$)-even($N+1$) daughter of each odd($Z-1$)-even($N+1$) proton "emitter" result in the transition between the lowest-energy 2^+ state and 0^+ ground state in the "daughter" nucleus. Therefore, the coincidence between βp and the $2^+\rightarrow 0^+$ γ-ray transition specific for a particular "daughter" nucleus, a "p-γ" coincidence, can be used to identify the mother, the βp precursor. This method can also be used to identify some of the odd(Z)-odd(N) precursors. It should be noted that the sum of the proton branching ratios ($b_{\beta p}$) to the excited states followed by the $2^+\rightarrow 0^+$ γ-ray transition in the "daughter" nucleus is larger than the EC branching ratio followed by βp emission. On the other hand, the transportation efficiency of a He-jet tape transport system (HJTTS) for the rare-earth or refractory nuclei is higher than the overall efficiency of an isotope separator on line (ISOL). Generally speaking, using the "p-γ" coincidence in combination with a HJTTS, the efficiency of measuring the βp specific for a particular rare-earth or refractory nucleus can be increased by a factor of 50 in comparison with that using the "x-p" coincidence in combination with an ISOL facility. Therefore, in our experiment the "p-γ" coincidence in combination with HJTTS was employed to identify the studied nuclei.

4 Results and discussion [13]

9 βp precursors[14—18] along the Z=0.743N+11.6 line (Fig. 2) have been identified for the first time by our group using the "p-γ" coincidence, including predicted drip-line nuclei ^{142}Ho and ^{128}Pm. The βp decays of 7 isotopes in the rare-earth region have been restudied. In particular, the βp decays from the ground state and an isomeric state in ^{143}Dy and ^{133}Sm have been observed and separated for the first time. As a by-product, the new data of 5 refractory nuclei[19—21] in the mass 90 region near N=Z line (Fig. 1(b) of Ref. [13]) have been published by our group, including the predicted "waiting point" nuclei in the rp-process ^{89}Ru and ^{98}Pd. The experimental results are summarized and compared with the predictions of some successful nuclear models.

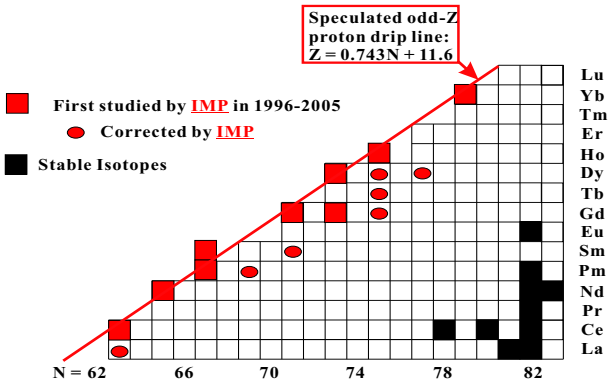

Fig. 2. Chart of the rare-earth nuclides on neutron deficient side.

4.1 Half-life

The experimental values of the half-lives of the 9 studied rare-earth nuclei are $1.1^{+}_{-}0.1$s (^{121}Ce), $0.65^{+}_{-}0.15$s (^{125}Nd), $1.0^{+}_{-}0.3$s(^{128}Pm), $0.55^{+}_{-}0.10$s (^{129}Sm), $1.1^{+}_{-}0.2$s (^{135}Gd), $2.2^{+}_{-}0.2$s (^{137}Gd), $0.6^{+}_{-}0.2$s (^{139}Dy), $0.4^{+}_{-}0.1$s (^{142}Ho), and $0.7^{+}_{-}0.2$s (^{149}Yb). The experimental results are consistent with the theoretical predictions[22—26] reasonably.

The experimental values of the half-lives of the 5 studied nuclei in the mass 90 region near N=Z line compared with the predictions of some successful nuclear models are listed in Table II of Ref. [13]. Except the half-life of ^{81}Zr, the experimental values in Table II of Ref. [13] are 5—10 times longer than the predictions given by Mo.ller et al[25]. A network calculation was made for the time integrated rp-process reaction flow during the x-ray burst at the typical conditions of temperature T_9=1.5 and density ρ=1.5×10^{6}g/cm^3[27]. We employed two sets of the nuclear input data: the standard one taken from Ref. [28] by Schatz. et al, and the present set in which our experimental β-decay half-lives for the four nuclei ^{93}Pd, ^{92}Rh, ^{89}Ru and ^{85}Mo were used to replace those in the standard data set. The only difference between these two data sets is the different half-lives for the four nuclei. The half-lives of the four nuclei in standard set are originally quoted from the theoretical predictions given by Mo.ller et al[25]. In order to make a comparison, the abundances of the waiting point nuclei ^{89}Ru and ^{93}Pd as functions of the processing time, are calculated with both present set of the nuclear input data and the standard set. The calculated abundances of ^{89}Ru and ^{93}Pd with the present experimental half-lives are larger than that with the standard predicted half-lives during the entire processing time, and the present experimental half-lives lead to about 4 times more products of these two waiting point nuclei around the peak abundances.

4.2 Spin, parity and deformation

The experimental values for the spins and parities of the 9 rare-earth nuclei extracted by fitting the measured βp energy spectrum and relative branching ratios to low-lying states in the "daughter" nucleus with a statistical model calculation[29] are listed in Table III of Ref. [13] and compared with the theoretical predictions of some successful nuclear models. In Table III of Ref. [13] it can be seen that the experimental spin-parity values of the 7 even(Z)-odd(N) nuclei are consistent with theoretical predictions reasonably. The theoretical determination of the ground-state spin and parity for an even-odd nucleus by means of the orbital occupied by the last neutron in the Nilsson diagram strongly depends on the nuclear deformation. Therefore, the consistency between the experimental spin-parity assignments and the predicted Nilsson diagrams in Refs. [25,30—32] is an indirect indication that the six even-odd nuclides ^{121}Ce, ^{125}Nd, ^{129}Sm, ^{135}Gd, ^{137}Gd, and ^{139}Dy are highly deformed with β_2 ∼0.3[33]. However, the experimental spin-parity assignments of the odd-odd nuclides ^{142}Ho and ^{128}Pm are inconsistent with almost all the theoretical predictions. Recently. the nuclear potential-energy surfaces (PES) for the two odd-odd nuclides were calculated by using a Woods-Saxon Strutinsky method[34]. In the calculated PES for the negative-parity configuration of ^{142}Ho a minimum at deformation parameters β_2=0.251 and γ=9.3° was found which corresponds to the configuration of $(\pi 7/2^-[523]\times\nu 7/2^+[404])7^-$, while in the calculated PES for the positive-parity configuration of ^{128}Pm a minimum at β_2=0.319 and γ=−0.8° was found which corresponds to the configuration of $(\pi 5/2^-[532]\times\nu 7/2^-[523])6^+$. The calculated PES for ^{142}Ho and ^{128}Pm are in good agreement with our experimental spin-parity assignments, and

indicate that both ^{142}Ho and ^{128}Pm also are highly deformed with $\beta_2 \sim 0.3$.

The experimental spin-parity assignments of the 5 nuclei in the mass 90 region near $N=Z$ line are $3/2^-$ (^{81}Zr), $1/2^+$ (^{85}Mo), $5/2^+$ or 7/2 (^{89}Ru), 9/2 (^{92}Rh), and $\geqslant 5$ (^{93}Pd), which are consistent with the theoretical predictions of some successful nuclear models[17,21—23] resonably except ^{85}Mo. The experimental spin-parity of ^{85}Mo is inconsistent with all the predictions. The inconsistency, most probably, is due to the fact that the nuclear deformation near ^{85}Mo varies dramatically, and therefore, is not easy to be reproduced by any model calculations.

4.3 Production reaction cross section

According to the measured counting rate of βp, the production reaction cross sections for the 9 rare-earth nuclei were estimated and are listed in Table V of Ref. [13]. On the other hand, the fusion-evaporation reaction cross section ($\sigma_{\rm fe}$) was calculated by using Alice [35] and HIVAP [36] code with normal input parameters. The calculated reaction cross sections also are listed in Table V of Ref. [13]. Average speaking, Alice code overestimates the $\sigma_{\rm fe}$ by one order of magnitude or two, and HIVAP code overestimates it by one order of magnitude approximately.

4.4 Recent results

The βp decay of ^{143}Dy was studied by Nischke et al in early 1980's, and the βp decay of ^{133}Sm was studied by Bogdanov et al in 1977 and followed by Wilmarth et al in 1985. All of them only used the ISOL facility to identify the βp precursors, and then could not be able to separate the βp decay of an isomeric state from that of the ground state in same isotope. Recently we restudied the βp decays of ^{143}Dy and ^{133}Sm by using the "p-γ" coincidence in combination with a HJTTS instead. Two components of the βp decay of ^{143}Dy have been found[37], one from the 1/2+ ground state and another from a 11/2− isomeric state. Similarly, we also observed the βp decay of the 1/2− ground state and a 5/2+ isomeric state in ^{133}Sm simultaneously, and separated one from another.

5 Perspective in near future

Now we are working in the region along the odd-Z proton drip line. The even-Z proton drip line around the rare-earth region is about 4-5 neutrons less than the odd-Z proton drip line (Fig. 3). One of major decay mode for the nuclei between these two lines is βp decay. Using the "p-γ" coincidence, we are able to study the βp decays in this uncultivated area, starting from the odd-Z proton drip line, and gradually reaching the even-Z proton drip line.

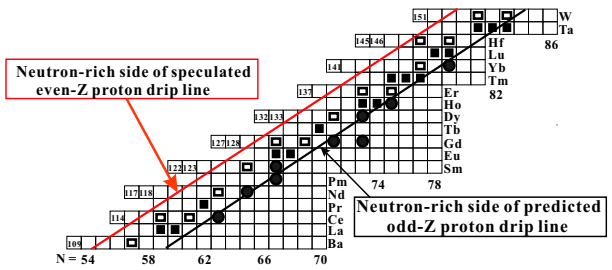

Fig. 3. Chart of the neutron-deficient nuclides in Z=56—74 region.

References

1 Bogdanov D D, Demyanov A V, Karnaukhov V A et al. Nucl. Phys., 1977, **A275**: 229—236
2 Schardt D, Larsson P O, Kirchner R et al. Proc. Intern. Conf. Atomic Masses and Fundamental Constants, 7th, Darmstadt-Seeheim, 1984, 229—233
3 Nitschke J M, Cable M D, Zeitz W D. Z. Phys., 1983, **A312**: 265—266
4 Nitschke J M, Wilmarth P A, Lemmertz P K et al. Z. Phys., 1984 **A316**: 249—250
5 Wilmarth P A, Nitschke J M, Lemmertz P K et al. Z. Phys.,1985, **A321**: 179—180
6 Wilmarth P A, Nitschke J M, Firestone R B et al. Z. Phys., 1986, **A325**: 485—486
7 Wilmarth P A, Nitschke J M, Vierinen K et al. Z. Phys., 1988, **A329**: 503—504
8 Nitschke J M, Wilmarth P A, Gilat J et al. Phys. Rev., 1988, **C37**: 2694—2703
9 Vierinen K S, Wilmarth P A, Nitschke J M et al. Phys. Rev., 1989, **C39**: 1972—1975
10 Firestone R B, Gilat J, Nitschke J M et al. Phys. Rev., 1991, **C43**: 1066-1085

11 Toth K S, Wilmarth P A, Nitschke J M et al. Phys. Rev., 1993, **C48**: 445—447
12 Hofmann S. Radiochim. Acta, 1995, **70/71**: 93—105
13 XU Shu-Wei, LI Zhan-Kui, XIE Yuan-Xiang et al. Phys. Rev., 2005, **C71**: 054318
14 XU Shu-Wei, XIE Yuan-Xiang, LI Zhan-Kui et al. Z. Phys., 1996, **A356**: 227—228
15 LI Zhan-Kui, XU Shu-Wei, XIE Yuan-Xiang et al. Phys. Rev., 1997, **C56**, 1157—1159
16 XU Shu-Wei, LI Zhan-Kui, XIE Yuan-Xiang et al. Phys. Rev., 1999, **C60**: 061302(R)
17 XU Shu-Wei, LI Zhan-Kui, XIE Yuan-Xiang et al. Phys. Rev., 2001, **C64**: 017301
18 XU Shu-Wei, LI Zhan-Kui, XIE Yuan-Xiang et al. Eur. Phys. J., 2001, **A12**: 1—4
19 HUANG Wen-Xue, MA Rui-Chang, XU Shu-Wei et al. Phys. Rev., 1999, **C59**: 2402—2405
20 LI Zhan-Kui, XU Shu-Wei, XIE Yuan-Xiang et al. Eur. Phys. J., 1999, **A5**: 351—352
21 XU Shu-Wei, LI Zhan-Kui, XIE Yuan-Xiang et al. Eur. Phys. J., 2001, **A11**: 375—377
22 Takahashi K, Yamada M, Kondoh T. At. Data Nucl. Data Tables, 1973, **12**: 101—142; Koyama S I, Takahashi K, Yamada M. Prog. Theor. Phys., 1970, **44**: 663
23 Horiguchi T, Tachibana T, Katakura J. Chart of the Nuclides 2000, Japanese Data Committee and Nuclear Data Center, 2000
24 Hirsch M, Staudt A, Muto K et al. At. Data Nucl. Data Tables, 1993, 53: 165—178
25 Möller P, Nix J R, Kratz K L. At. Data Nucl. Data Tables, 1997, **66**: 131—343
26 Herndl H, Brown A B. Nucl. Phys., 1997, **A627**: 35—52
27 Wallace R K, Woosley S E. Astrophys. J. Suppl., 1981, **389**: 45—53
28 Schatz H, Aprahamina A, Görres J et al. Phys. Rep., 1998, **294**: 167—263
29 Hagberg E, Hardy J C, Schmeing H et al. Nucl. Phys., 1983, **A395**: 152—164
30 Arseniev D A, Sobiczewski A, Soloview V G. Nucl. Phys., 1969, **A139**: 269—276
31 Bengtsson T, Ragnarsson I. Nucl. Phys., 1985, **A436**: 14—80; Firestone R B. Table of Isotopes, 8th ed. 1996, Vol.II, Appendix H, H-7 and H-8
32 Audi G, Bersillon O, Blachot J et al. Nucl. Phys., 1997 **A624**: 1—124
33 Möller P, Nix J R, Myers W D et al. At. Data Nucl. Data Tables, 1995, **59**: 185—381
34 Nazarewicz W, Dudek J, Bengtsson R et al. Nucl. Phys., 1985, **A435**: 397—447
35 Winn W G, Gutbrod H H, Blann M. Nucl. Phys., 1987, **A188**: 423—429
36 Reisdorf W. Z Phys., 1981, **A300**: 227—238; Veselsky M. Z. Phys., 1997, **A356**: 403—410
37 XU Shu-Wei, XIE Yuan-Xiang, LI Zhan-Kui et al. Eur. Phys. J., 2003, **A16**: 347—351

稀土区近滴线的β缓发质子衰变*

徐树威[1)]　李占奎　谢元祥　郭文涛

(中国科学院近代物理研究所　兰州　730000)

摘要　简要回顾了自20世纪70年代以来实验研究稀土区β缓发质子衰变的历史. 综合报道了在过去10年内中科院近物所实验研究稀土区近滴线核的β缓发质子衰变的进展, 主要包括首次观测沿奇Z质子滴线的9种新核素的β缓发质子衰变以及rp-过程中两种等待点核的衰变新数据, 并将这些结果与不同的核模型理论计算进行了比较和讨论. 最后对今后的工作进行了初步展望.

关键词　缓发质子衰变　稀土区　质子滴线　等待点核

* 国家自然科学基金(10375078)资助

1) E-mail: xsw@impcas.ac.cn